

Transition Metal Chemistry

Rhodium(I) macrocyclic and cage-like structures containing diphosphine bridging ligands.

--Manuscript Draft--

Manuscript Number:	
Full Title:	Rhodium(I) macrocyclic and cage-like structures containing diphosphine bridging ligands.
Article Type:	Research Article
Keywords:	macromolecular complexes; rhodium; diphosphines; luminescence; DFT calculations; catalysis
Corresponding Author:	Laura Rodriguez Universitat de Barcelona SPAIN
Corresponding Author Secondary Information:	
Corresponding Author's Institution:	Universitat de Barcelona
Corresponding Author's Secondary Institution:	
First Author:	Julià Arcau
First Author Secondary Information:	
Order of Authors:	Julià Arcau Montserrat Ferrer Elisabet Aguiló Laura Rodriguez
Order of Authors Secondary Information:	
Funding Information:	
Abstract:	<p>Three series of rhodium organometallic complexes, mono- (1c, 2c, 5c, 6c), di- (1a-6a) and tetranuclear (1b, 5b, 6b), containing six different diphosphines (1,1'-bis(diphenylphosphino)methane or dppm (1), 1,2-bis(diphenylphosphino)ethane or dppe (2), 1,4-bis(diphenylphosphino)butane or dppb (3), bis(diphenylphosphino)acetylene or dppa (4), 1,2-bis(diphenylphosphino)benzene or dppbz (5) and 4,5-bis(diphenylphosphino)-9,9'-dimethylxanthene or xantphos (6) were successfully synthesised. These Rh(I) complexes were characterised by conventional techniques. The influence of the flexibility/rigidity of these P-donor ligands was carefully analysed, including their effect on both synthesis and catalysis. The luminescent properties of the dinuclear and tetranuclear complexes were investigated and only those containing dppa, dppbz and xantphos displayed luminescence. Structures of dinuclear complexes were modelled by using DFT methods in order to elucidate the most possible conformation.</p> <p>The different types of complexes were applied in the catalytic hydrogenation of (E)-4-phenylbut-3-en-2-one, showing high activity and similar catalytic behaviour. No cooperative effect could be inferred.</p>

[Click here to view linked References](#)

Rhodium(I) macrocyclic and cage-like structures containing diphosphine bridging ligands.

Julià Arcau, Montserrat Ferrer, Elisabet Aguiló and Laura Rodríguez.*

*Departament de Química Inorgànica i Orgànica, Secció de Química Inorgànica,
Universitat de Barcelona, Martí i Franquès 1-11, E-08028 Barcelona, Spain*

Phone.: +34934039130. Fax: +34934907725.

e-mail: laura.rodriguez@qi.ub.es

Abstract

Three series of rhodium organometallic complexes, mono- (**1c**, **2c**, **5c**, **6c**), di- (**1a-6a**) and tetranuclear (**1b**, **5b**, **6b**), containing six different diphosphines (1,1'-bis(diphenylphosphino)methane or dppm (**1**), 1,2-bis(diphenylphosphino)ethane or dppe (**2**), 1,4-bis(diphenylphosphino)butane or dppb (**3**), bis(diphenylphosphino)acetylene or dppa (**4**), 1,2-bis(diphenylphosphino)benzene or dppbz (**5**) and 4,5-bis(diphenylphosphino)-9,9'-dimethylxanthene or xantphos (**6**) were successfully synthesised. These Rh(I) complexes were characterised by conventional techniques. The influence of the flexibility/rigidity of these P-donor ligands was carefully analysed, including their effect on both synthesis and catalysis. The luminescent properties of the dinuclear and tetranuclear complexes were investigated and only those containing dppa, dppbz and xantphos displayed luminescence. Structures of dinuclear complexes were modelled by using DFT methods in order to elucidate the most possible conformation.

The different types of complexes were applied in the catalytic hydrogenation of (*E*)-4-phenylbut-3-en-2-one, showing high activity and similar catalytic behaviour. No cooperative effect could be inferred.

Keywords: macromolecular complexes, rhodium, diphosphines, luminescence, DFT calculations, catalysis

Introduction

1 The use of transition metal-based self-assembly processes has emerged as one of
2
3
4 the most efficient ways to build artificial supramolecular structures [1-3]. Typically, a
5
6 metal complex with two or more available coordination sites is reacted with an
7
8 appropriately designed multifunctional ligand to give the product in one step in high
9
10 yield.

11
12
13 Square-planar Pd(II) and Pt(II) complexes have been commonly used to prepare
14
15 metallocsupramolecules which contain square or near orthogonal angles in their
16
17 geometry [1-8]. However, other metals have also been used in these reactions. In
18
19 particular, Rh(I) and Ir(I) units have been explored in the synthesis of bi- [9-14] and
20
21 three-dimensional compounds [15-18], and they are of great interest due to their
22
23 luminescent behaviour [19], their potential catalytic activity [20-25] and they could also
24
25 be very useful in molecular recognition studies [26, 27], among others.

26
27
28 In recent years, bimetallic complexes have been used in homogeneous catalysis
29
30 as an effective tool for promoting organic transformations [28, 29]. Bimetallic catalysts
31
32 can display cooperative effects, because of the proximity between the metal centres,
33
34 leading to reactivities and selectivities that cannot be attained using their corresponding
35
36 monometallic counterparts [30, 31].

37
38 Over the last few decades, bidentate ligands have been widely employed to
39
40 improve selectivities, activities, and stabilities of metal-complex-based homogeneous
41
42 catalysts [32-35]. The key to optimize the performance of a certain specimen in a
43
44 catalytic reaction is to adjust the electronic and steric properties together with the
45
46 topology exhibited by the ligands.

47
48 The use of binucleating ligands with ligand isolated donor sets is one of the
49
50 more recent developments where two metal centres are held in close proximity to
51
52 cooperatively catalyse a given organic transformation [31]. Cooperative effects that
53
54
55
56
57
58
59
60
61
62
63
64
65

1 have been observed in bimetallic systems usually occur through electronic and/or spatial
2 interactions. In particular, concerning the reactivity of group 9 bimetallic catalysts, it is
3 important to underline the work reported by Stanley and co-workers with highly
4 selective and active dirhodium hydroformylation catalyst, $[\text{Rh}_2(\text{norbornadiene})(\text{P4})]$,
5 where P4 is the binucleating tetraphosphine-based ligand,
6 $(\text{Et}_2\text{PCH}_2\text{CH}_2)(\text{Ph})\text{PCH}_2\text{P}(\text{Ph})(\text{CH}_2\text{CH}_2\text{PEt}_2)$ [36]. Another example was shown by
7
8 Barbara A. Messerle and co-workers with a dual metal catalyst system (Rh and Ir) using
9 cationic Rh(I) and Ir(I) complexes of the type $[\text{M}(\text{bpm})(\text{CO})_2]\text{BArF}_4$ (where M = Rh or
10 Ir, bpm = *bis*(1-pyrazolyl)methane, and $\text{BArF}_4 = \text{tetrakis}[3,5\text{-bis}(\text{trifluoromethyl})\text{-}$
11 phenyl]borate) which is observed to be a highly efficient catalyst for the two step
12 intramolecular dihydroalkoxylation reaction of alkyne diols in the formation of
13 spiroketals [37]. The two metal centres worked cooperatively to provide greater
14 efficiencies than the individual monometallic complexes for the concurrent cyclization
15 of alkyne diols.
16
17

18
19
20
21
22
23
24
25
26
27
28
29
30
31
32
33
34
35
36
37
38
39
40
41
42
43
44
45
46
47
48
49
50
51
52
53
54
55
56
57
58
59
60
61
62
63
64
65

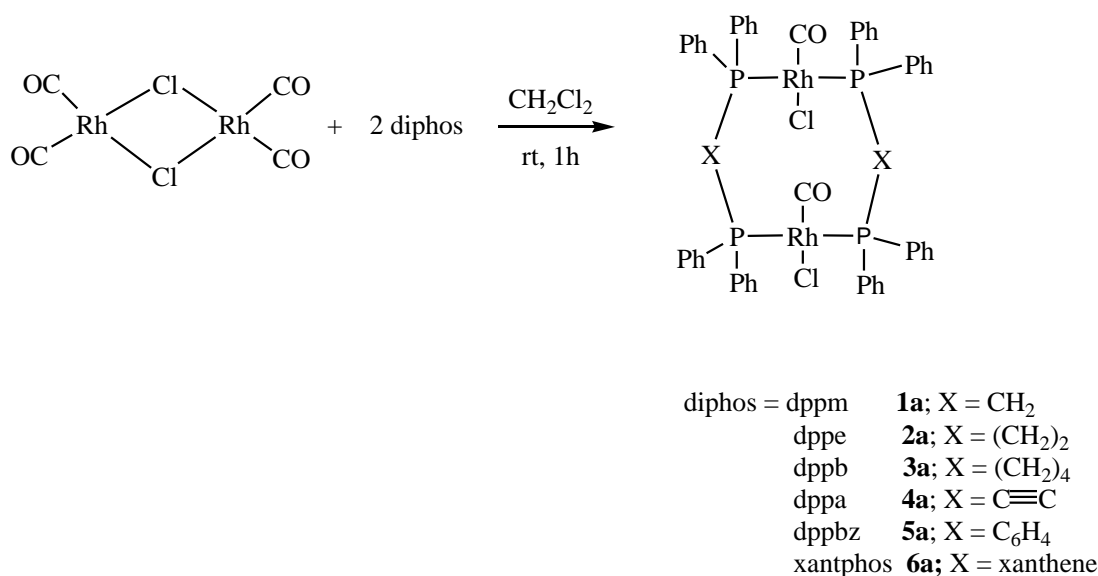
Van Leeuwen and co-workers claimed the involvement of bimetallic catalytic species using wide bite angle diphosphine ligands in particular in carbonylation reactions [38, 39].

For all the reasons above we decided to go on with our previous work based on the synthesis of bi- and three-dimensional rhodium structures containing diphosphine ligands as linkers between metal atoms [40]. Their catalytic behaviour on hydrogenation reaction was analysed and the possible cooperative effects on these processes was studied and compared with the parent mononuclear rhodium complexes.

Results and Discussion

Synthesis of rhodium dinuclear complexes

[RhCl(CO)₂]₂ reacted with six different diphosphines **1-6** (Rh:P = 1:2) in dichloromethane at room temperature for 1h (Scheme 1). The reaction was monitored by ³¹P-NMR until the disappearance of the free diphosphine signal, which was *ca.* 40-60 ppm downfield shifted upon coordination to the metal atom. The corresponding dinuclear complexes [RhCl(CO)₂]₂(μ-diphos)₂ (**1a-6a**) were obtained in high yields after concentration of the solution and precipitation with hexane.



Scheme 1. Synthesis of dinuclear complexes **1a-6a**.

Compounds **1a** and **3a** were previously described following different synthetic procedures [41-43]. Evidence for the proposed structures was obtained from IR, ¹H-NMR and ³¹P-NMR spectroscopy and MS spectrometry. ³¹P-NMR spectra present different profiles due to the existence of different isomers and their relative stabilities as depicted in Figure 1. **4a** displayed two set of signals with different intensities, showing close chemical shifts (24.0 ppm and 24.6 ppm) and the same coupling constant value (J(P-Rh) = 124 Hz). This behaviour has been already reported in the literature for

1 closely related dinuclear rhodium derivatives [44], and attributed to the existence of
2 different conformational isomers arising from the relative disposition of the phosphine
3 backbones (chair/boat or parallel/antiparallel in Figures 2 and 3) isomers and also, from
4 the relative orientation of the carbonyl and chloride ligand in both rhodium centres (*syn*
5 and *anti* isomers in Figures 2 and 3).
6
7
8
9

10 Some broadening of the signals was only observed for **1a** and could be due to a
11 dynamic process that involves the coordination-decoordination of the diphosphines, as
12 dynamic process that involves the coordination-decoordination of the diphosphines, as
13 previously observed for its analogue three-dimensional complex **1b** [40].
14
15
16
17

18 The sharp and well defined doublet exhibited by **2a**, **5a-6a** could be due to the
19 fact that these diphosphines form exclusively one complex in solution, or that several
20 isomers exist in a fast equilibrium at the temperature of study.
21
22
23
24
25
26

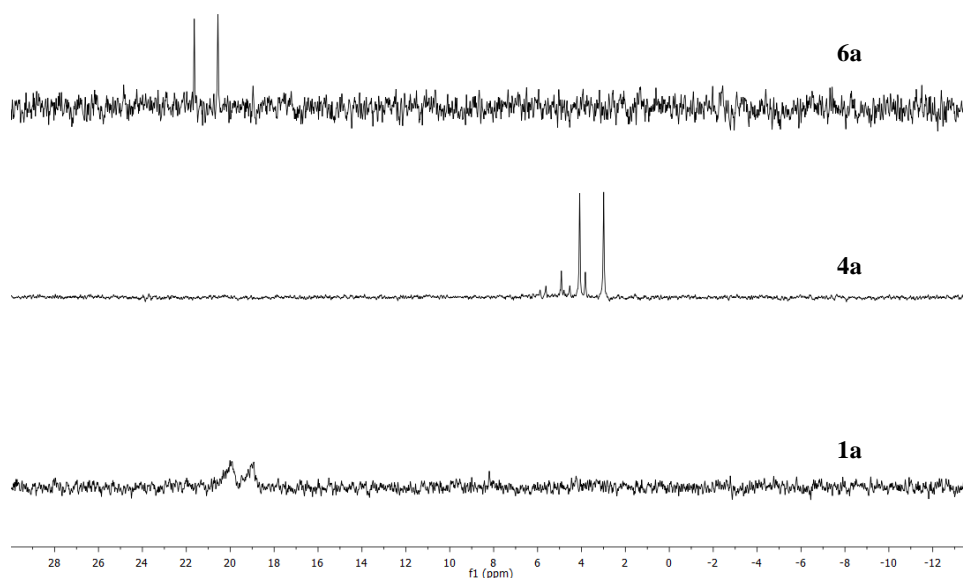


Figure 1. ^{31}P -NMR spectra of **1a**, **4a** and **6a** in CDCl_3 .

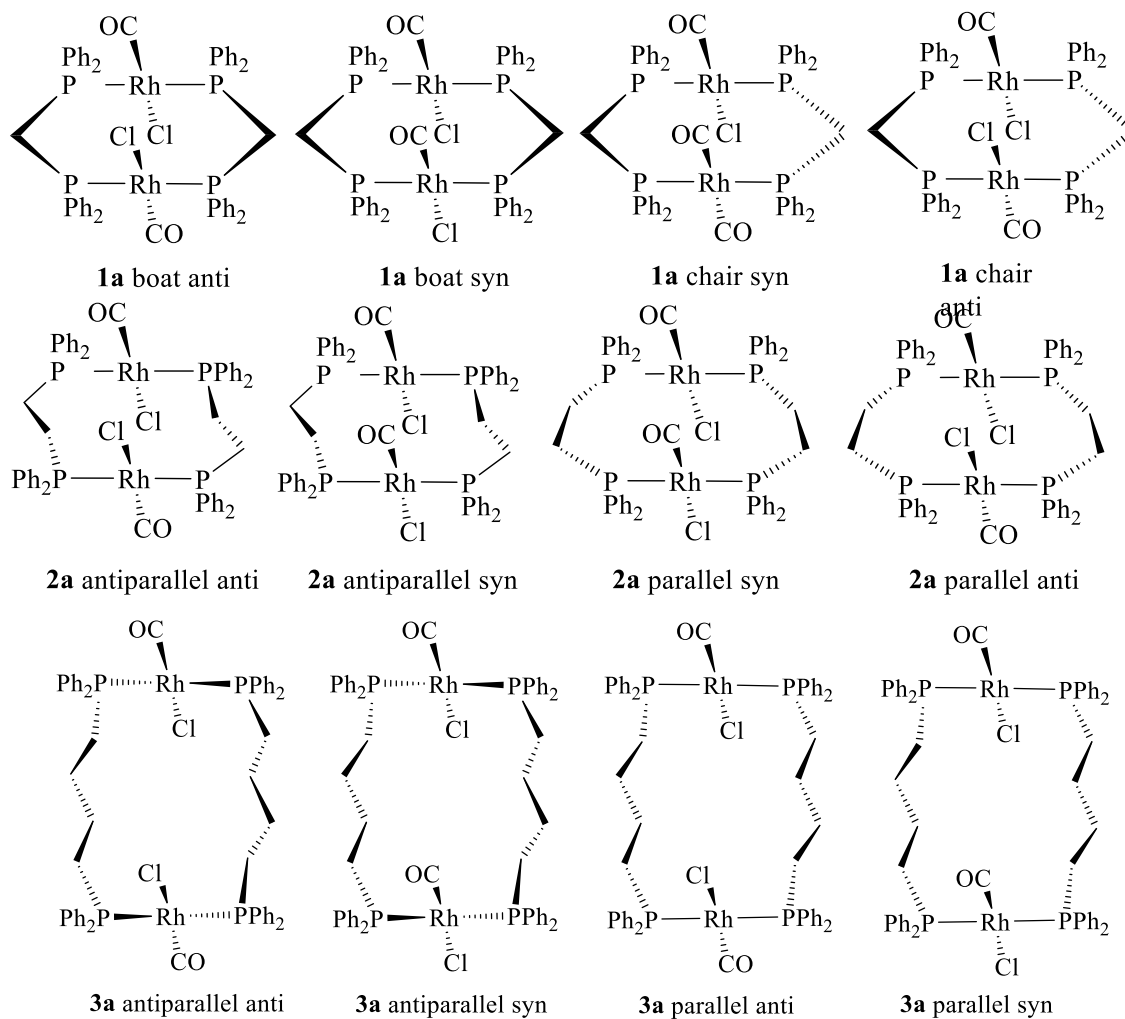


Figure 2. Different possible conformers expected for **1a-3a** complexes.

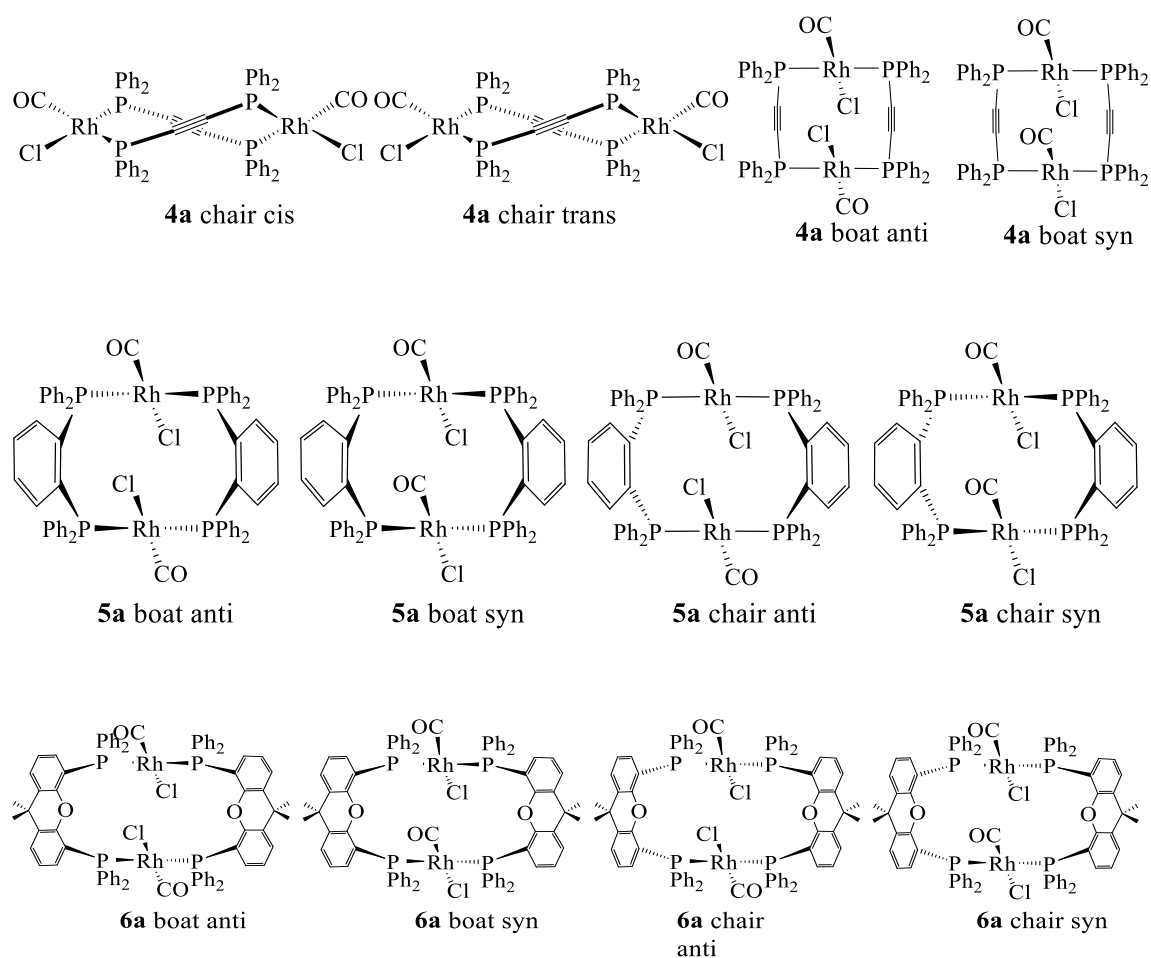


Figure 3. Different possible conformers expected for **4a-6a** complexes.

Structure optimization of the dinuclear complexes

As indicated above, a wide range of different conformations could be plausible for our face-to-face (*trans-P*) complexes depending both on the *syn/anti* or *cis/trans* (only for **4a**) disposition of the chloride and carbonyl ligands coordinated to the metal atoms and the relative arrangement of the backbone chain of the diphosphine with respect to an imaginary Rh-Rh edge (chair/boat for complexes **1a** and **4-6a** or parallel/antiparallel for **2a** and **3a**).

In order to find out the different possible isomers and the most stable in each case, we have performed theoretical calculations at the DFT level, using the RB3LYP

hybrid functional (see experimental section). The optimized structures are displayed in Figures S1-S6 and the calculated minimum energy in all cases is shown in Table 1.

Table 1. Calculated minimum energies for the different isomers of **1a-6a** compounds.

The most stable isomer (considered to have an energy of 0.0 kcal/mol) is highlighted in bold.

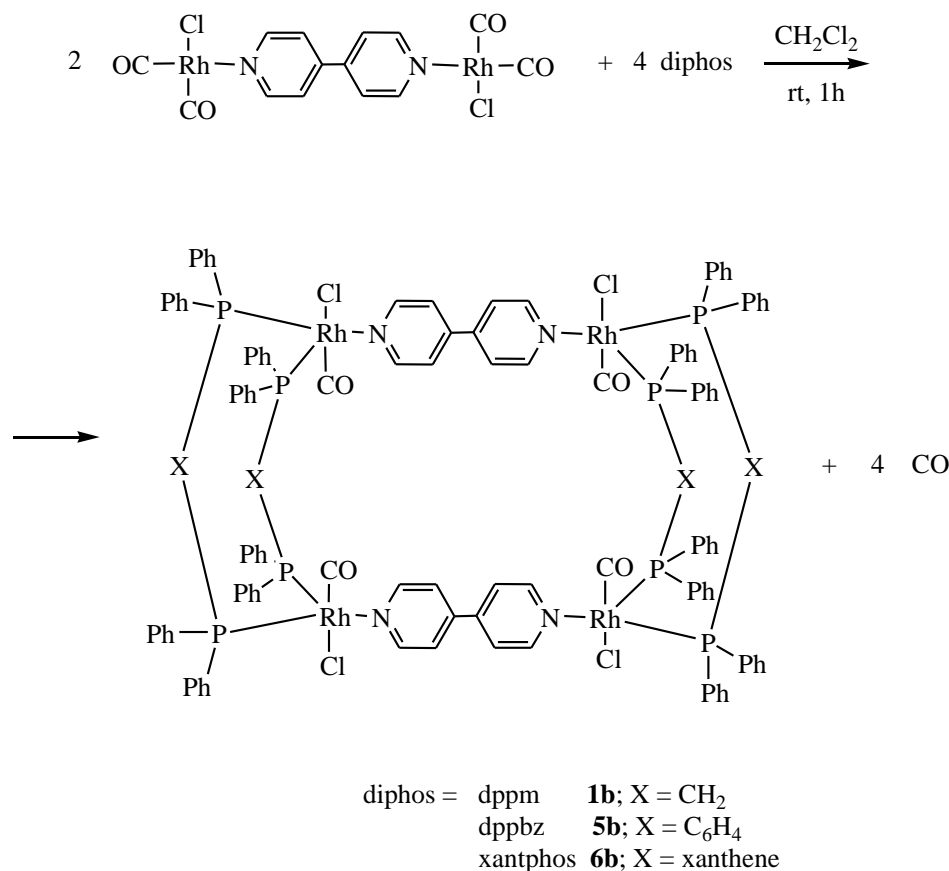
Compound	Energy (kcal/mol)	
1a chair	<i>syn</i>	<i>anti</i>
	16.7	0.0
1a boat	<i>syn</i>	<i>anti</i>
	4.5	13.9
2a antiparallel	<i>syn</i>	<i>anti</i>
	6.4	14.3
2a parallel	<i>syn</i>	<i>anti</i>
	10.7	0.0
3a antiparallel	<i>syn</i>	<i>anti</i>
	0.0	12.1
3a parallel	<i>syn</i>	<i>anti</i>
	6.2	7.3
4a chair	<i>cis</i>	<i>trans</i>
	8.2	11.6
4a boat	<i>syn</i>	<i>anti</i>
	0.9	0.0
5a chair	<i>syn</i>	<i>anti</i>
	14.3	1.7
5a boat	<i>syn</i>	<i>anti</i>
	3.4	0.0
6a chair	<i>syn</i>	<i>anti</i>
	1.8	0.0
6a boat	<i>syn</i>	<i>anti</i>
	11.6	10.7

Inspection of Table 1 shows a clear dependence of the nature of the diphosphine upon the stability of the corresponding isomers. However, the obtained values do not allow establishing a direct correlation between length, bulkiness and/or flexibility of the phosphine backbone chain and the energetically favoured isomer. In spite of this, a general preference for the *anti* disposition of the chloride and carbonyl ligands is observed although in some cases the difference between both conformations is too small to be considered reliable (see for example **4a** boat and **6a** chair).

The rhodium atom presents, in all cases, a square planar geometry and the inner cavities are observed to be in the range *ca.* 3.5 x 6.3 Å for **1a**, 5.1 x 5.6 Å for **2a**, 7.2 x 5.4 Å for **3a**, 3.0 x 5.1 Å for **5a** and 4.1 x 7.1 Å for **6a** for all possible conformations. A particular case is **4a** whose cavity presents a completely different size in the case of chair conformation (3.4 x 7.5 Å) and boat (5.3 x 5.4 Å). Moreover, the only square-like cavity is the one corresponding to the acetylide derivative **4a**, in boat conformation.

Synthesis of rhodium tetranuclear complexes

Following the same experimental procedure previously reported by some of us [40] (Scheme 2), we planned the synthesis of different cage-like rhodium structures. Our main goal was the formation of new three-dimensional complexes with different inner size cavities in order to explore their influence on different applications, such as in catalysis.



Scheme 2. Synthesis of tetranuclear complexes **1b**, **5b** and **6b**.

1 [RhCl(CO)₂]₂(μ-4,4'-bipy) reacted with the corresponding diphosphine (Rh:P =
2 1:2) in dichloromethane for 1h. Actually compounds **1b** [40], **5b** and **6b** were efficiently
3 isolated, while the use of the other diphosphines (dppe, dppb, dppa) did not give rise to
4 the formation of the desired products. The high rigidity of the dppa probably prevents
5 the cage-type structure and the high flexibility of dppe and dppb favours the formation
6 of oligomers.
7
8
9

10
11
12
13 ³¹P-NMR spectra of **5b** and **6b** complexes exhibit one broad doublet centred at
14 20 - 60 ppm with a Rh-P coupling constant of *ca.* 135 Hz. The value of these coupling
15 constants is in the same range than the previously reported for **1b** [40].
16
17
18
19

20
21 IR spectra show more complex ν(C≡O) stretching vibration patterns with respect
22 to the two IR bands observed for the precursor, [RhCl(CO)₂]₂(μ-4,4'-bipy) (Figures S7
23 and S8) [40]. Each band splits in two with an additional lower energy vibration. This
24 shift is in agreement with a higher retro-donation effect from the rhodium centre to the
25 antibonding molecular orbital of the carbonyl ligand because of the loss of one CO
26 ligand upon diphosphine coordination. Maldi/TOF mass analyses evidenced peaks
27 consistent with the tetranuclear structure.
28
29
30
31
32
33
34
35
36

37 38 **Photophysical characterization** 39

40 Absorption and emission spectra of compounds **1a**, **2a**, **4a-6a**, **1b**, **5b** and **6b**
41 were recorded at 1·10⁻⁵ M in dichloromethane. The results are summarised in Table 2
42 and Figures 4 and 5.
43
44
45
46

47 The spectra of both bimetallic and tetrametallic complexes are dominated by
48 strong absorption bands attributed to intraligand (IL) π → π* transitions, with
49 diphosphine-based π → π* transitions in the near-UV region between 280 - 300 nm
50 along with a relatively weak, broad band in the visible range (between 350 and 450 nm).
51 The broad visible bands are similar to the metal-to-ligand charge-transfer (MLCT)
52 transitions observed in rhodium complexes containing π-acceptor ligands [45, 46], in
53
54
55
56
57
58
59
60
61
62
63
64
65

which the charge transfer character stems from interactions between filled metal d orbitals and antibonding ligand π^* orbitals.

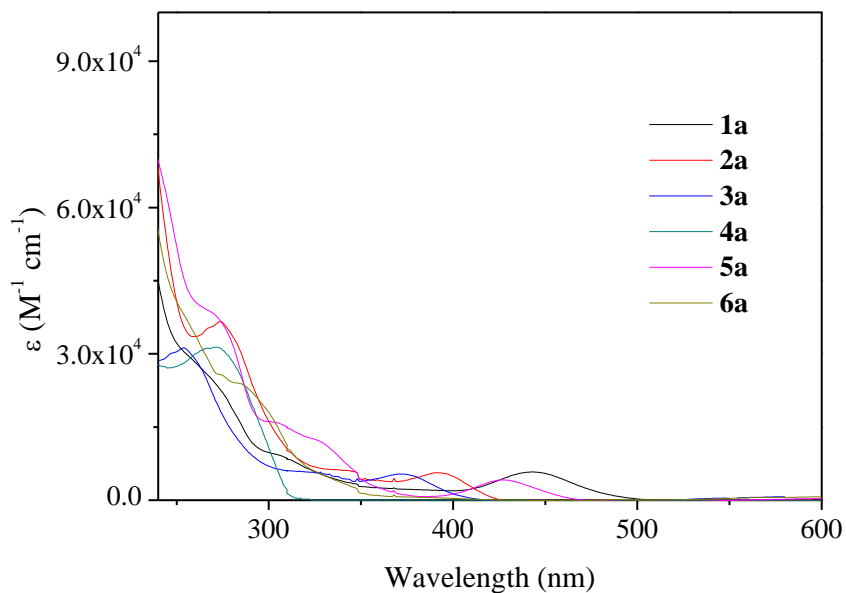


Figure 4. Absorption spectra of the dinuclear complexes (**1a**, **2a**, **4a-6a**) at $1 \cdot 10^{-5}$ M in dichloromethane.

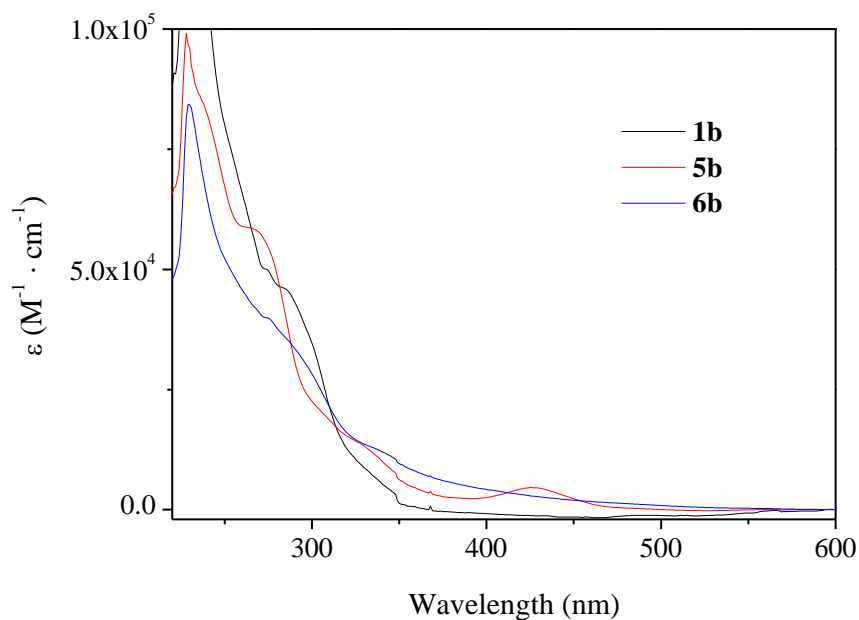


Figure 5. Absorption spectra of **1b**, **5b** and **6b** complexes at $1 \cdot 10^{-5}$ M in dichloromethane.

The MLCT transition is observed to be less favoured for the tetrametallic derivatives being only clearly defined for the dppbz derivative, **5b**, probably due to the higher aromaticity and electron deficiency of the system due to the presence of the benzene unit.

Table 2. Absorption and emission wavelengths (nm) of complexes **1a-6a** ($\lambda_{\text{exc}}=280$ nm) and **1b-6b** ($\lambda_{\text{exc}}=274$ nm) at $1 \cdot 10^{-5}$ M concentration. ^a $\lambda_{\text{exc}}=333$ nm

Compounds	Absorption ($\epsilon \times 10^{-3}, \text{M}^{-1} \cdot \text{cm}^{-1}$)	Emission ($\text{CH}_2\text{Cl}_2, 298 \text{ K}$)
1a	443 (5.8), 324 (6.1), 263 (27.2)	-
2a	390 (5.6), 343 (7.1), 275 (36.1)	-
3a	375 (3.21), 328 (5.4), 254 (31.2)	-
4a	270 (31.3)	340, 410
5a	428 (4.1), 325 (12.5), 272 (37.6)	-
6a	331 (5.0), 283 (24.0)	335
1b	335sh (7.1), 285 (45.9)	335
5b	428 (4.6), 325 (14.3), 265 (58.6)	-

6b	335sh (12.9), 280 (37.8)	335, 415 ^a
-----------	--------------------------	-----------------------

The only emissive dinuclear species are **4a** and **6a** (dppa and xantphos derivatives, Figure 6). Excitation spectra collected at the emission maxima match the lowest energy absorption band being indicative of an intraligand emission origin. It should be noticed that, as displayed in Figure 6, the emission spectrum of **4a** presents two different bands. The vibronically well-resolved highest energy emission band is in agreement with the involvement of the acetylene group on this transition. The broad structureless lowest energy band can be tentatively attributed to metal centered transitions, since $d\sigma^* \rightarrow p\sigma$ excited states are common for dinuclear Rh(I) complexes coordinated by bidentate ligands [47].

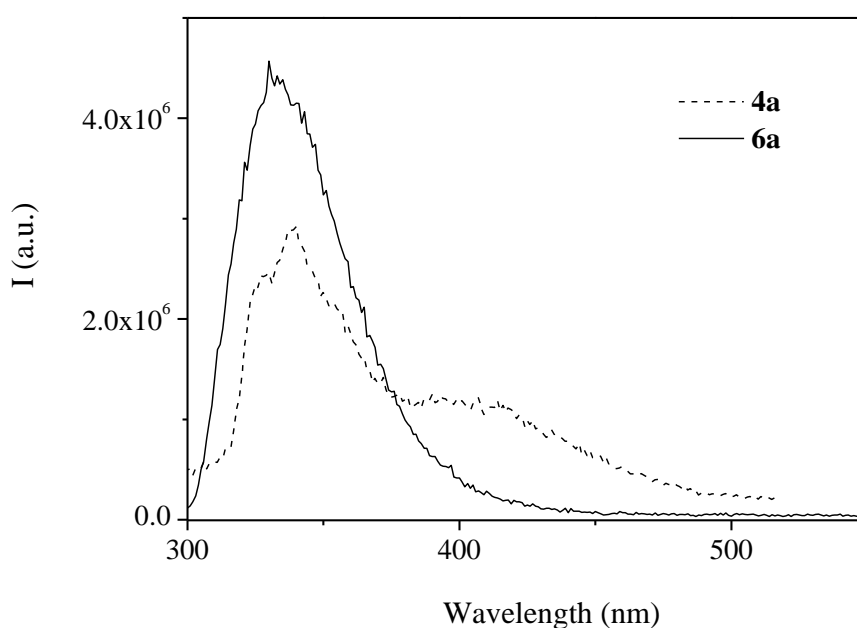


Figure 6. Emission spectra of **4a** (dashed line) and **6a** (solid line) in dichloromethane solution (dashed line) upon excitation the samples at 280 nm.

Compounds **1b** and **6b** (dppm and xantphos derivatives) displayed a broad luminescence at *ca.* 350 nm upon excitation the samples at the intraligand absorption band (Figure 7). The small Stokes' shift (*ca.* 5000 cm^{-1}) suggests a singlet emissive IL origin state. An additional lower energy emission is observed for **6b** when the sample is excited at the MLCT transition being indicative of the different origin transitions. Excitation spectra collected at the maxima are in agreement with these assignments (Figure S9-S10). No emission was displayed by complex **5b**.

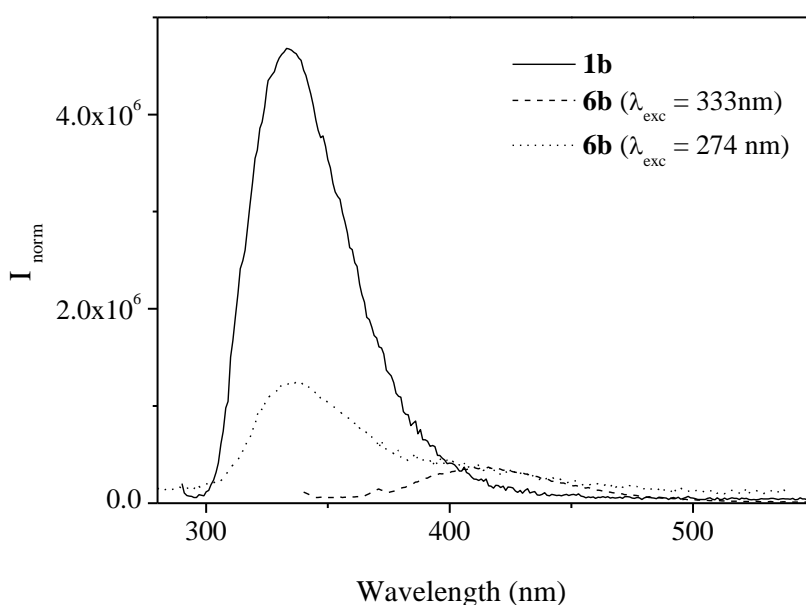
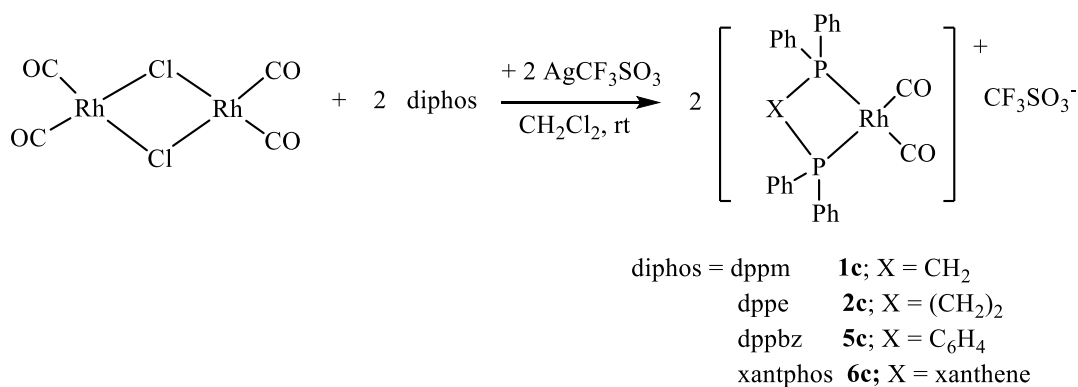


Figure 7. Emission spectra of **1b** (solid line) and **6b** in dichloromethane solution (dashed and dotted line).

Synthesis of rhodium mononuclear complexes

Mononuclear derivatives were also synthesised in order to compare the catalytic behaviour of the different complexes. For this, the reaction of $[\text{RhCl}(\text{CO})_2]_2$ with the appropriate diphosphine in stoichiometric conditions (after extraction of the chloride ligand by addition of silver triflate) was applied to give the monomeric species **1c**, **2c**, **5c** and **6c** (Scheme 3).



Scheme 3. Synthesis of monometallic complexes **1c**, **2c**, **5c** and **6c**.

The corresponding reaction with dppb gave rise to the formation of different species in equilibrium whose ³¹P-NMR signals showed similar chemical shifts, preventing the isolation of pure **3c**. Moreover, the rigidity of the alkynyl group of the diphosphine dppa blocks that the diphosphine could act as a chelating ligand and consequently precludes the formation of the mononuclear complex **4c** [45, 49].

IR spectra of the isolated complexes, in particular the region corresponding to ν(C≡O) absorptions, revealed the expected *cis*-CO arrangement in agreement with the reported data [38, 48].

Catalytic hydrogenation

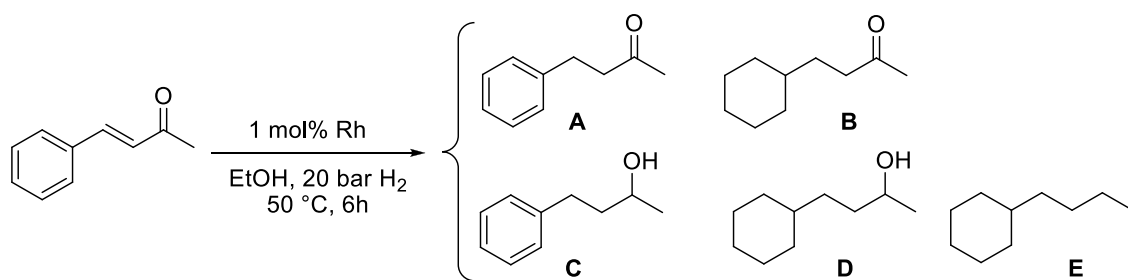
The dinuclear complexes **1a**, **2a** and **4a-6a** were used as catalytic precursors in the hydrogenation reaction of the polyfunctional substrate (*E*)-4-phenylbut-3-en-2-one, in order to analyse their ability towards the reduction of the different groups present on the same substrate. **3a** was not used for this purpose since it was observed to decompose rapidly in solution. Under the conditions indicated in Scheme 4, we could not observe important differences among the different Rh(I) complexes leading to full conversion (entries 1-5 in Table 3), except for **4a** which was less active (42% conversion, entry 3), probably due to an induction period corresponding to the hydrogenation of the C≡C

1 triple bond present in the ligand skeleton, leading to the same catalytic system generated
2 by **2a**. The hydrogenation mainly gave 4-phenylbutan-2-one (**A** in Scheme 4) in all the
3 cases, being **6a** the most active system (able to hydrogenate the aromatic ring), which
4 gave up to 14% of 4-cyclohexylbutan-2-one (entry 5). The system **1a** was the only
5 giving butylcyclohexane (**E** in Scheme 4) as by-product coming from the hydrogenative
6 dehydration process of alcohol **D**.
7
8
9
10
11
12

13 In order to selectively attain one hydrogenated product, smoother conditions
14 were applied. Actually, 4-phenylbutan-2-one, **A**, was exclusively obtained under 5 bar
15 of dihydrogen for 3h of reaction (entry 6). Using the most active catalytic system, **6a**,
16 under harsher conditions (at 80 °C or 40 bar H₂) no differences in the reactivity were
17 observed (entry 5 vs 7 and 8). With a higher load of catalyst and longer time, only **A**
18 and **C** were obtained in a ratio of 77:23 (entry 9). The highest amount of **C** was
19 obtained under 40 bar H₂ for 24h (entry 10).
20
21
22
23
24
25
26
27
28
29

30 We also tested the tetranuclear complexes **1b** and **6b**. Xanthphos-based complex
31 (**6b**) was slightly more active than **1b**, giving 92% of **A** and 8% of **C**, while **1b** led
32 exclusively to the formation of **A**. Both catalytic trends are similar to those obtained
33 with the corresponding dinuclear complexes, **1a** (under smooth conditions) and **6a**
34 respectively (entries 5-6 vs 11-12), pointing to a lower activity of the tetranuclear
35 systems in comparison with the dinuclear ones.
36
37
38
39
40
41
42
43
44

45 The monometallic complex **2c** used as catalytic precursor, gave the same
46 reactivity trend than the related bimetallic system **2a** (entry 13 vs 2). The similar
47 reactivity exhibited by the dinuclear complexes **1a**, **2a**, **5a** and **6a** and the monometallic
48 complex **2c**, together with the lower activity of the tetranuclear complexes **1b** and **6b**,
49 seems to suggest that the active catalytic species are mononuclear complexes generated
50 *in situ* under catalytic conditions from the corresponding dinuclear ones.
51
52
53
54
55
56
57
58
59
60
61
62
63
64
65



Scheme 4. Hydrogenation of *(E)*-4-phenylbut-3-en-2-one catalysed by Rh(I) complexes

Table 3. Hydrogenation of (*E*)-4-phenylbut-3-en-2-one catalysed by polynuclear Rh complexes. Conditions: 1 mmol of (*E*)-4-phenylbut-3-en-2-one, 0.01 mmol of Rh, 20 bar H₂, 20 mL of ethanol, 50 °C, 2h. Full conversion for all the systems except for **4a**.^a Determined by GC and ¹H NMR using decane as internal standard. ^b 42% conversion ^c Under 5 bar H₂ for 3h. ^d At 80 °C. ^e Under 40 bar H₂. ^f 0.02 mmol of Rh for 24h. ^g Under 40 bar H₂ for 24h.

Entry	Complex	Selectivity (%) ^a
		A/B/C/D/E
1	1a	87/4/7/-/2
2	2a	85/8/7/-/-
3 ^b	4a	95/5/-/-/-
4	5a	88/5/7/-/-
5	6a	82/14/4/-/-
6 ^c	1a	100/-/-/-/-
7 ^d	6a	85/13/2/-/-
8 ^e	6a	86/12/2/-/-
9 ^f	6a	77/23/-/-/-
10 ^g	6a	48/49/3/-/-
11	1b	100/-/-/-/-
12	6b	92/8/-/-/-
13	2c	85/9/6/-/-

Conclusions

1 The reaction of six different diphosphines with Rh(I) organometallic precursors
2
3
4 led to the formation of five new dinuclear (**1a**, **2a**, **4a-6a**) and two tetranuclear (**5b**, **6b**)
5
6 complexes. The use of the high flexible dppb ligand precluded the formation of the
7
8 complexes in pure form and rapid decomposition was observed in solution. The use of
9
10 more rigid diphosphines (dppbz and xantphos) favoured the formation of three-
11
12 dimensional cage-like derivatives.
13
14

15
16 The compounds displayed very weak emissions in dichloromethane with some
17
18 intraligand luminescence observed for **4a**, **6a**, **1b** and **6b** and an additional ³MLCT band
19
20 for **6b**.
21
22

23 Theoretical calculations at density functional level (DFT) carried out to know
24
25 the most stable conformation of the dinuclear complexes have shown a clear influence
26
27 of the backbone of the diphosphine on the stability of the different conformers.
28
29

30 Mono-, di- and tetrametallic complexes were assayed as catalytic precursors for
31
32 the hydrogenation of (*E*)-4-phenylbut-3-en-2-one. The similar behaviour observed
33
34 between polynuclear and monometallic complexes suggests that the active catalytic
35
36 species are mononuclear moieties generated under the catalytic conditions used in these
37
38 studies.
39
40
41
42
43
44
45
46
47
48
49
50
51
52
53
54
55
56
57
58
59
60
61
62
63
64
65

Experimental Section

General

All manipulations were performed under prepurified N₂ using standard Schlenk techniques. All solvents were distilled from appropriate drying agents. Compounds [RhCl(CO)₂]₂ [49], [RhCl(CO)₂]₂(μ-bipy) [40], 1,1'-bis(diphenylphosphino)methane (dppm) [50], 1,2-bis(diphenylphosphino)ethane (dppe) [50] 1,4-bis(diphenylphosphino)butane (dppb) [50], [RhCl(CO)₂]₂(μ-dppm)₂ [51] and ([RhCl(CO)₂]₂(μ-4,4'-bipy))₂(μ-dppm)₄ (**1b**) [40] were synthesised as described previously. Compound 4,4'-bipyridine (Avocado, 98%), *trans*-4-phenyl-3-butene-2-one (Janssen Chimica, 99%), 1,2-bis(diphenylphosphino)-acetylene (dppa), 4,5-bis(diphenylphosphino)-9,9'-dimethylxanthene (xantphos), 1,2-bis(diphenylphosphino)benzene (dppbz) were used as received.

Infrared spectra were recorded on an FT-IR 520 Nicolet spectrophotometer. ³¹P{¹H}-NMR (δ(85% H₃PO₄) = 0.0 ppm), and ¹H-NMR (δ(TMS) = 0.0 ppm) spectra were obtained on a Bruker DXR 250, Varian Inova 300 and Varian Mercury 400 spectrometers. ES(+) mass spectra were recorded on a Fisons VG Quatro spectrometer. Absorption spectra were recorded on a Varian Cary 100 Bio UV-spectrophotometer and emission spectra on a Horiba-Jobin-Yvon SPEX Nanolog spectrofluorimeter. GC analyses were carried out on an Agilent GC6890 with a flame ionization detector, using a SGE BPX5 column composed by 5% of phenylmethylsiloxane. ES(+) mass spectra were recorded with a Fisons VG Quatro spectrometer. Maldi/TOF spectra were recorded on a Maldi Tof Voyager DE STR (Applied Biosystems) instrument.

Molecular modelling was carried out using Spartan'10 V1.1.0 for Mac as software. DFT calculations were carried out with the Spartan software using the B3LYP hybrid functional [52]. The basis set was chosen as follows: for Rh LANL2DZ was used

[53] while for the remaining atoms the 6-31G basis [54] was used. The structures were previously optimised at MM+ molecular mechanics level.

Synthesis and Characterization

Synthesis of $[\text{RhCl}(\text{CO})]_2(\mu\text{-dppm})_2$ (**1a**).

Similar procedure previously described in the literature [51] was followed but dichloromethane instead of cyclohexane was used as solvent. Yield: 74 %. ^{31}P -NMR (121.42 MHz, 298K, CDCl_3): 19.6 ppm (d, $^1\text{J}(\text{Rh-P}) = 115$ Hz). ^1H -NMR (300 MHz, 298K, CDCl_3): 7.67-7.27 (m, 40H, Ph), 3.96 (br, 4H, P- CH_2 -P). ESI-MS(+) m/z : 1102.9 (M + H^+ , calc.: 1102.5), 1045.0 (M - 2CO + H^+ , calc.: 1046.1), 1010.0 (M - 2CO - Cl, calc.: 1010.0). IR (KBr, cm^{-1}) 1970 s, $\nu(\text{C}\equiv\text{O})$.

Synthesis of $[\text{RhCl}(\text{CO})]_2(\mu\text{-dppe})_2$ (**2a**).

A dichloromethane solution (5 mL) of dppe (103 mg, 0.26 mmol) was added to a solution (5 mL) of $[\text{RhCl}(\text{CO})]_2$ (50 mg, 0.13 mmol) in the same solvent. After 1h of stirring the bright orange solution became dark red. The solution was concentrated to ca. 4 mL and hexane (20 mL) was added. The obtained pale orange solid was filtered, washed with hexane and vacuum dried. Yield: 75 % (109 mg). ^{31}P -NMR (121.42 MHz, 298K, CDCl_3): 57.5 ppm (d, $^1\text{J}(\text{Rh-P}) = 101$ Hz). ^1H -NMR (300 MHz, 298K, CDCl_3): 8.78-7.38 (m, 40H, Ph), 2.38 (br, 4H, P-(CHH_a) $_2$ -P), 2.27 (br, 4H, P-(CH_bH) $_2$ -P). ESI-MS(+) m/z : 501.0 (M - 2CO - 2Cl, calc.: 501.3). IR (KBr, cm^{-1}): 1986 vs, $\nu(\text{C}\equiv\text{O})$.

Synthesis of $[\text{RhCl}(\text{CO})]_2(\mu\text{-dppa})_2$ (**4a**).

A similar procedure that described for **2a** was used in the synthesis of **4a** but dppa instead of dppe was used to obtain a pale yellow solid. Yield: 70 %. ^{31}P -NMR (121.42 MHz, 298K, CDCl_3): 3.6 ppm (d, $^1\text{J}(\text{Rh-P}) = 133$ Hz). ^1H -NMR (300 MHz, 298K, CDCl_3): 7.87-7.25 (m, Ph). ESI-MS(+) m/z : 497.0 (M - 2CO - 2Cl, calc.: 497.2). IR (KBr, cm^{-1}): 2105 m, $\nu(\text{C}\equiv\text{C})$; 1986 vs, $\nu(\text{C}\equiv\text{O})$.

Synthesis of $[\text{RhCl}(\text{CO})]_2(\mu\text{-dppbz})_2$ (**5a**).

1 Similar procedure described for **2a** was used in the synthesis of **5a** using dppbz instead
2
3 of dppe to obtain a pale yellow solid. Yield: 70%. ^{31}P -NMR (121.42 MHz, 298K,
4
5 CDCl_3): 62.3 ppm (d, $^1\text{J}(\text{Rh-P}) = 134$ Hz). ^1H -NMR (300 MHz, 298K, CDCl_3): 7.59-
6
7 6.83 (m, Ph + P- C_6H_4 -P). ESI-MS(+) m/z : 995.0 ($[\text{M} - 3 \text{ Ph}]^+$, calc.: 994.9). IR (KBr,
8
9 cm^{-1}): 1973 vs, $\nu(\text{C}\equiv\text{O})$.

Synthesis of $[\text{RhCl}(\text{CO})]_2(\mu\text{-xantphos})_2$ (**6a**).

10 Similar procedure described for **2a** was used in the synthesis of **6a** by using xantphos
11
12 instead of dppe to obtain an orange solid. Yield: 80 %. ^{31}P -NMR (121.42 MHz, 298K,
13
14 CDCl_3): 21.1 ppm (d, $^1\text{J}(\text{Rh-P}) = 131$ Hz). ^1H -NMR (300 MHz, 298K, CDCl_3): 7.59-
15
16 7.07 (m, 56H, Ph + $\text{H}_{\text{Arom, Xanthene}}$), 1.85-1.55 (m, 12H, CH_3). ESI-MS(+) m/z : 1491.0 (M
17
18 + H^+ , calc.: 1490.9), 1426.1 (M - CO - Cl^- , calc.: 1426.6), 710.0 (M - 2 Cl^- , calc.:
19
20 709.6). IR (KBr, cm^{-1}): 1986 vs, $\nu(\text{C}\equiv\text{O})$.

Synthesis of $([\text{RhCl}(\text{CO})]_2(\mu\text{-4,4'-bipy}))_2(\mu\text{-dppbz})_4$ (**5b**).

21 A dichloromethane solution (5 mL) of dppbz (37 mg, 0.08 mmol) was added to a
22
23 solution (5 mL) of $[\text{RhCl}(\text{CO})]_2(\mu\text{-bipy})$ (22 mg, 0.04 mmol) in the same solvent. After
24
25 1 h of stirring the orange solution turned bright yellow. The solution was concentrated
26
27 to ca. 4 mL and hexane (15 mL) was added. The obtained pale orange solid was filtered,
28
29 washed with hexane and vacuum dried. Yield: 80% (44 mg). ^{31}P -NMR (121.42 MHz,
30
31 298K, acetone- d_6): 61.7 ppm (d, $^1\text{J}(\text{Rh-P}) = 133$ Hz). ^1H -NMR (300 MHz, 298K,
32
33 acetone- d_6): 8.90 (br, 8H, $\text{H}_{\alpha\text{-pyr}}$), 8.05-7.02 (m, 104H, Ph + P- C_6H_4 -P + $\text{H}_{\beta\text{-pyr}}$).
34
35 Maldi/TOF m/z : 2131.1 (M - dppz - 4CO - 2Cl + H^+ , calc.: 2131.0), 1047.0
36
37 ($[\text{RhCl}(\text{CO})]_2(\mu\text{-dppbz})_2 - 2\text{Ph} - \text{Cl} + \text{CH}_3\text{CN}$, calc.: 1047.1). IR (KBr, cm^{-1}): 2097 s,
38
39 2059 s, 2012 vs, 1978 vs, $\nu(\text{C}\equiv\text{O})$; 1612 s, $\nu(\text{C}=\text{N})$.
40
41
42
43
44
45
46
47
48
49
50
51
52
53
54
55
56
57
58
59
60
61
62
63
64
65

Synthesis of $[\text{RhCl}(\text{CO})]_2(\mu\text{-4,4'}\text{-bipy})_2(\mu\text{-xantphos})_4$ (**6b**).

1 Similar procedure described for **5b** was used in the synthesis of **6b** by using xantphos
2 instead of dppbz. Yield: 85%. ^{31}P -NMR (121.42 MHz, 298K, acetone- d_6): 20.9 ppm (d,
3
4
5
6 $^1\text{J}(\text{Rh-P}) = 137$ Hz). ^1H -NMR (300 MHz, 298K, acetone- d_6): 8.94 (br, 8H, $\text{H}_{\alpha\text{-pyr}}$), 8.08
7
8
9 (m, 8H, $\text{H}_{\beta\text{-pyr}}$), 7.92-6.83 (m, 112H, Ph + $\text{H}_{\text{Arom,Xanthene}}$), 2.30 (m, 24H, $(\text{CH}_3)_2\text{Xanthene}$).
10
11
12
13
14
15
16
17
18
19
20
21
22
23
24
25
26
27
28
29
30
31
32
33
34
35
36
37
38
39
40
41
42
43
44
45
46
47
48
49
50
51
52
53
54
55
56
57
58
59
60
61
62
63
64
65
Maldi/TOF m/z : 1599.2 (M - 2Cl^- - CO, calc.: 1599.1), 1586.2 (M - 2Cl^- - 2CO , calc.:
1586.10), 1572.2 (M - 2Cl^- - 3CO , calc.: 1572.1), 1557.2 (M - 2Cl^- - 4CO , calc.:
1557.1), 1543.3 (M - 2Cl^- - 4CO - 2CH_3 , calc.: 1543.2), 1525.2 (M - 2Cl^- - 4CO - 4
CH₃, calc.: 1525.2), 1510.2 (M - 2Cl^- - 4CO - 6CH_3 , calc.: 1510.2), 1373.9 (M -
xantphos - 2Cl^- + CH_2Cl_2 + H_2O , calc.: 1373.8), 1353.1 (M - xantphos - 2Cl^- +
MeOH + $2\text{H}_2\text{O}$, calc.: 1353.1), 1322.0 (M - xantphos - 2Cl^- , calc.: 1322.0). IR (KBr,
cm⁻¹): 2099 s, 2012 s, 1986 m, 1966 w, $\nu(\text{C}\equiv\text{O})$; 1612 m, $\nu(\text{C}=\text{N})$.

Synthesis of $[\text{Rh}(\text{CO})_2(\text{dppm})](\text{OTf})$ (**1c**).

Solid AgOTf (37 mg, 0.14 mmol) was added to a stirred solution of $[\text{Rh}(\mu\text{-Cl})(\text{CO})_2]_2$
(25 mg, 0.06 mmol) and dppm (49 mg, 0.13 mmol) in CH_2Cl_2 (20 mL). After 15 min
stirring, AgCl was eliminated by filtration through Celite, the solution was concentrated
and hexane (50 mL) was added and a yellow-orange solid was obtained. Yield: 90% (75
mg). ^{31}P -NMR (121.42 MHz, 298K, CDCl_3): 19.4 ppm (d, $^1\text{J}(\text{Rh-P}) = 114$ Hz). ^1H -
NMR (300 MHz, 298K, CDCl_3): 7.70-7.11 (m, 20H, Ph), 4.08 (br, 1H, P- $\text{CHH}_a\text{-P}$), 3.57
(br, 1H, P- $\text{CH}_b\text{H-P}$). ESI-MS(+) m/z : 515.3 (M^+ - CO, calc.: 515.0). IR (KBr, cm⁻¹)
1970 s, $\nu(\text{C}\equiv\text{O})$; 1101, 1030 (OTf).

Synthesis of $[\text{Rh}(\text{CO})_2(\text{dppe})](\text{OTf})$ (**2c**).

Similar procedure described for **1c** was used in the synthesis of **2c** by using dppe instead
of dppm to obtain a pale yellow solid. Yield: 92%. ^{31}P -NMR (121.42 MHz, 298K,
 CDCl_3): 57.6 ppm (d, $^1\text{J}(\text{Rh-P}) = 132$ Hz). ^1H -NMR (300 MHz, 298K, CDCl_3): 7.33-

7.11 (m, 20H, Ph), 2.11 (br, 4H, P-CH₂CH₂-P). ESI-MS(+): 453.2 (M⁺ - CO - Ph, calc.: 453.2). IR (KBr, cm⁻¹) 1972 s, ν(C≡O); 1101, 1031 (OTf).

Synthesis of [Rh(CO)₂(dppbz)](OTf) (**5c**).

Similar procedure described for **1c** was used in the synthesis of **5c** by using dppbz instead of dppm to obtain a pale yellow solid. Yield: 94%. ³¹P-NMR (121.42 MHz, 298K, CDCl₃): 62.4 ppm (d, ¹J(Rh-P) = 134 Hz). ¹H-NMR (300 MHz, 298K, CDCl₃): 7.38-6.75 (m, 24H, Ph). ESI-MS(+): 501.3 (M⁺ - CO - Ph, calc.: 501.3). IR (KBr, cm⁻¹) 1970 s, ν(C≡O); 1103, 1032 (OTf).

Synthesis of [Rh(CO)₂(xantphos)](OTf) (**6c**).

Similar procedure described for **1c** was used in the synthesis of **6c** by using xantphos instead of dppm to obtain a pale yellow solid. Yield: 90%. ³¹P-NMR (121.42 MHz, 298K, CDCl₃): 36.7 ppm (d, ¹J(Rh-P) = 123 Hz). ¹H-NMR (300 MHz, 298K, CDCl₃): 7.83-7.42 (m, 26H, Ph), 1.74 (s, 6H, CH₃). ESI-MS(+): 710.1 (M⁺ - CO, calc.: 710.1). IR (KBr, cm⁻¹) 1974 s, ν(C≡O); 1101, 1029 (OTf).

Catalytic hydrogenation procedure

(*E*)-4-phenyl-but-3-en-2-one (146 mg, 1.0 mmol) was added to a stirred solution of Rh catalyst (0.01 mmol of rhodium: 6 mg for **1a**, **2a**, **4a** and **5a**; 7.5 mg for **6a**; 6 mg for **2c**; 6.3 mg for **1b**) in ethanol (20 mL) in the presence of decane (142 mg, 1.0 mmol) as internal standard. The solution was then pressurised with H₂ (between 5 and 40 bar) at 50 °C during 6h. The crude solution was filtered off through Celite and analysed by GC/MS.

Acknowledgements

1 Authors would like to thank Dr. Isabelle Favier and Prof. Montserrat Gómez
2
3
4 from the Centre National de la Recherche Scientifique (CNRS) and the Université Paul
5
6 Sabatier in Toulouse (France) for the catalytic experiments. Financial support from the
7
8 Ministerio de Economía y Competitividad of Spain (Projects CTQ2012-31335 and
9
10 CTQ2015-65040-P) are also acknowledged.
11
12
13
14
15

Supporting Information Available

16
17
18
19 Ball and spoke model of the calculated structures (DFT-B3LYP) for the different
20
21 possible isomers of **1a** (Figure S1); Ball and spoke model of the calculated structures
22
23 (DFT-B3LYP) for the different possible isomers of **2a** (Figure S2); Ball and spoke
24
25 model of the calculated structures (DFT-B3LYP) for the different possible isomers of
26
27 **3a** (Figure S3); Ball and spoke model of the calculated structures (DFT-B3LYP) for the
28
29 different possible isomers of **4a** (Figure S4); Ball and spoke model of the calculated
30
31 structures (DFT-B3LYP) for the different possible isomers of **5a** (Figure S5); Ball and
32
33 spoke model of the calculated structures (DFT-B3LYP) for the different possible
34
35 isomers of **6a** (Figure S6); IR spectrum of **5b** (Figure S7); IR spectrum of **6b** (Figure
36
37 S8); Normalised excitation spectra of compounds **4a** and **6a** in $1 \cdot 10^{-5}$ M
38
39 dichloromethane solutions. $\lambda_{em} = 340$ nm (Figure S9); Normalised excitation spectra of
40
41 compounds **1b** and **6b** in $1 \cdot 10^{-5}$ M dichloromethane solutions. $\lambda_{em} = 340$ nm (black and
42
43 red line) and 413 (blue line) (Figure S10).
44
45
46
47
48
49
50
51
52
53
54
55
56
57
58
59
60
61
62
63
64
65

References

1. Cook TR, Zheng YR, Stang PJ (2013) *Chem Rev* 113:734
2. Cook TR, Zheng YR, Stang PJ (2015) *Chem Rev* 115:7001
3. Smulders MMJ, Riddell IA, Browne C, Nitschke JR (2013) *Chem Soc Rev* 42:1728
4. Ferrer M, Pedrosa A, Rodríguez L, Rossell O, Vilaseca M (2010) *Inorg Chem* 49:9438
5. Angurell I, Ferrer M, Gutiérrez A, Martínez M, Rocamora M, Rodríguez L, Rossell O, Lorenz Y, Engeser M (2014) *Chem Eur J* 20:14473.
6. Ferrer M, Gutiérrez A, Rodríguez L, Rossell O, Ruiz E, Engeser M, Lorenz Y, Schilling R, Gómez-Sal P, Martín A (2012) *Organometallics* 31:1533
7. Alvariño C, Pía E, García MD, Blanco V, Fernández A, Peinador C, Quintela JM (2013) *Chem Eur J* 19:15329
8. Ferrer M, Gómez-Bautista D, Gutiérrez A, Orduña-Marco G, Oro LA, Pérez-Torrente JJ, Rossell O, Ruiz E (2016) *Organometallics* 35:336
9. Ferrer M, Gómez-Bautista D, Gutiérrez A, Miranda JR, Orduña-Marco G, Oro LA, Pérez-Torrente JJ, Rossell O, García-Orduña P, Lahoz FJ (2014) *Inorg Chem* 53:1699
10. Forniés J, Gómez J, Lalande E, Moreno MT (2004) *Chem Eur J* 10:888
11. Wang H, Guo XQ, Zhong R, Lin YJ, Zhang PC, Hou XF (2009) *J Organomet Chem* 694:3362
12. Han YF, Lin YJ, Jia WG, Jin GX (2009) *Dalton Trans* 2009, 2077-2080
13. Álvarez-Vergara MC, Casado MA, Martín ML, Lahoz FJ, Oro LA, Pérez-Torrente JJ (2005) *Organometallics* 24:5929
14. Wang GL, Lin YJ, Jin GX (2011) *Chem Eur J* 17:5578
15. Han YF, Jia WG, Lin YJ, Jin GX (2008) *J Organomet Chem* 693:546
16. Grote Z, Bonazzi S, Scopelliti R, Severin K (2006) *J Am Chem Soc* 128:10328
17. Han YF, Lin YJ, Weng LH, Berke H, Jin GX (2008) *Chem Commun* 350-352

18. Govindaswamy P, Lindner D, Lacour J, Süß-Fink G, Therrien B (2007) Dalton
Trans 4457-4463
19. Tran NT, Stork JR, Pham D, Chancellor CJ, Olmstead MM, Fettinger JC, Balch AL
(2007) Inorg Chem 48:7998
20. Escárcega-Bobadilla MV, Rodríguez-Pérez L, Teuma E, Serp P, Masdeu-Bultó AM,
Gómez M (2011) Catal Lett 141:808
21. Giustra ZX, Ishibashi JSA, Li SY (2016) Coord Chem Rev 314:134
22. Delgado-Rebollo M, Prieto A, Pérez PJ (2014) Chem Cat Chem 6:2047
23. Sarmentero MA, Fernández-Pérez H, Zuidema E, Bo C, Vidal-Ferran A, Ballester P
(2010) Angew Chem Int Ed 49:7489
24. Besset T, Norman DW, Reek JNK (2013) Adv Synth Catal 355:348
25. Li Y, Wang Z, Ding K (2015) Chem Eur J 21:16387
26. Vargiu AV, Magistrato A (2012) Inorg Chem 51:2046
27. Mirtschin S, Krasniqi E, Scopelliti R, Severin K (2008) Inorg Chem 47:6375
28. Park J, Hong S (2012) Chem Soc Rev 41:6931
29. Wauchwalter P, Rose J, Braunstein P (2015) Chem Rev 115:28
30. Ho JHH, Wagler J, Willis AC, Messerle BA (2011) Dalton Trans 40:11031
31. Bratko I, Gómez M (2013) Dalton Trans 42:10664
32. Terrade FG, Lutz M, Reek JNH (2013) Chem Eur J 19:10458
33. Kokan Z, Kirin SI (2013) Eur J Org Chem 8154-8161
34. Sanhes D, Gual A, Castellón S, Claver C, Gómez M, Teuma E (2009) Tetrahedron:
Asymmetry 20:1009
35. Bravo MJ, Ceder RM, Muller G, Rocamora M (2013) Organometallics 32:2632
36. Matthews RC, Howell DK, Peng WJ, Train SG, Treleaven WD, Stanley GG (1996)
Angew Chem Int Ed Engl 35:2253
37. Ho JHH, Hodgson R, Wagler J, Messerle BA (2010) Dalton Trans 39:4062

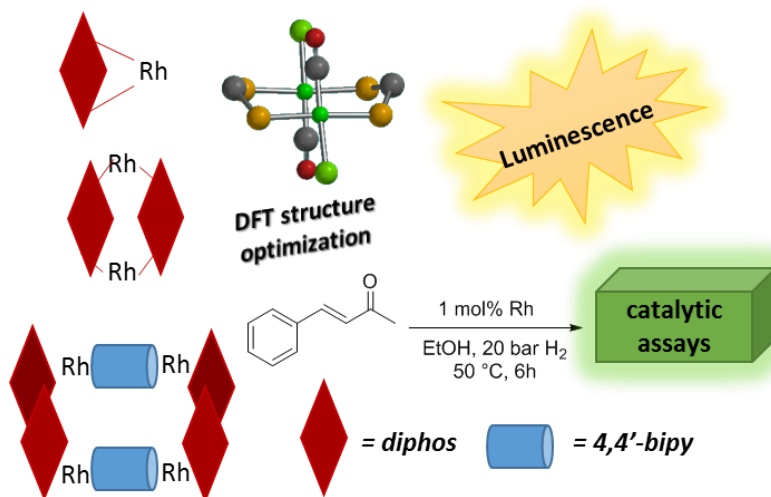
38. Freixa Z, Kamer PCJ, Lutz M, Spek AL, van Leeuwen PWNM (2005) *Angew Chem Int Ed* 44:4385
39. Feliz M, Freixa Z, van Leeuwen PWNM, Bo C (2005) *Organometallics* 24:2608
40. Rodríguez L, Ferrer M, Rossell O, Coco S (2009) *J Organomet Chem* 694:3951
41. Lamb G, Clarke M, Slawin AMZ, Williams B, Key L (2007) *Dalton Trans* 5582-5589
42. Lamb GW, Clarke ML, Slawin AMZ, Williams B (2008) *Dalton Trans* 4946-4950
43. Cowie M, Dwight SK (1980) *Inorg Chem* 19:209
44. López-Vallbuena JM, Escudero-Adan EC, Benet-Buchholz J, Freixa Z, van Leeuwen PWNM (2010) *Dalton Trans* 39:8560
45. de Pater BC, Fröhous HW, Vrieze K, de Gelder R, Baerends EJ, McCormack D, Lutz M, Spek AL, Hartl F (2004) *Eur J Inorg Chem* 1675-1686
46. Kunkely H, Vogler A (1999) *J Organomet Chem* 577:358
47. Indoli MT, Chiorboli C, Sandola F (2007) *Top Curr Chem* 280:215
48. Youssef TE (2010) *Polyhedron* 29:1776
49. Rojas S, Murcia-Mascarós S, Terrero P, García Fierro JL (2001) *New J Chem* 25:1430
50. Hewertso W, Watson HR (1962) *J Chem Soc* 1490
51. Mague J, Mitchener JP (1969) *Inorg Chem* 8:119
52. a) Becke AD (1993) *J Chem Phys* 98:5648; b) Lee C, Yang W, Parr RG, *Rev Phys B* 37:785
53. a) Wadt WR, Hay PJ (1985) *J Chem Phys* 82:284; b) Hay PJ, Wadt WR (1985) *J Chem Phys* 82:299
54. Hehre WJ, Ditchfield R, Pople JA (1972) *J Chem Phys* 56:2257

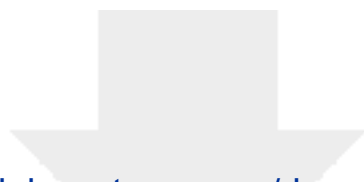
Rhodium(I) macrocyclic and cage-like structures containing diphosphine bridging ligands.

Julià Arcau, Montserrat Ferrer, Elisabet Aguiló and Laura Rodríguez.*

*Departament de Química Inorgànica i Orgànica, Secció de Química Inorgànica,
Universitat de Barcelona, Martí i Franquès 1-11, E-08028 Barcelona, Spain
Phone.: +34934039130. Fax: +34934907725.
e-mail: laura.rodriguez@qi.ub.es*

Three series of 1D, 2D and 3D rhodium complexes were successfully synthesised and their emission properties were analysed. The large number of isomeric forms of the 2D were analysed by DFT methods. Their use in catalytic hydrogenation of (*E*)-4-phenylbut-3-en-2-one was studied showing high selectivity towards the formation of 4-phenylbutan-2-one.





Click here to access/download
Supplementary Material
Rhodium 2D_3D_SI.docx

